ISSN 1070-3632, Russian Journal of General Chemistry, 2015, Vol. 85, No. 10, pp. 2252–2261. © Pleiades Publishing, Ltd., 2015.
Original Russian Text © A.N. Eryomin, A.V. Abakshonok, V.E. Agabekov, A.Yu. Panarin, S.N. Terekhov, 2015, published in Zhurnal Obshchei Khimii, 2015, Vol. 85, No. 10, pp. 1620–1629.

Formation of a Gold/Silver-Containing Composite

A. N. Eryomin[a], A. V. Abakshonok[a], V. E. Agabekov[a], A. Yu. Panarin[b], and S. N. Terekhov[b]

[a] *Institute of New Materials Chemistry, National Academy of Sciences of Belarus,*
ul. F. Skoriny 36, Minsk, 2200141 Belarus
e-mail: yan47@mail.ru

[b] *Stepanov Institute of Physics, National Academy of Sciences of Belarus, Minsk, Belarus*

Received April 2, 2015

Abstract—Preparation of the Au/Ag composite in the 1 : 1 water–ethanol mixture in the presence of poly-*N*-vinylpyrrolidone has been optimized; the so prepared composite is applicable in the absorption spectroscopy based on the effect of plasmon resonance energy transfer. Of the studied cationic, anionic, and non-ionic polymer, only the 340 kDa poly-*N*-vinylpyrrolidone induced the formation of a monodisperse Au/Ag sol with the average hydrodynamic diameter of the particles of ≈73 nm. The composite structure built of the polymer core covered with the Au/Ag nanoparticles has likely formed. The prepared composite binds both anionic and cationic metal porphyrins preserving the efficient transfer of the plasmon resonance energy.

Keywords: gold, silver, nanoparticle, nanocomposite, resonance light scattering, plasmon resonance, energy transfer

DOI: 10.1134/S1070363215100060

Silver and gold nanoparticles are promising for applications in nanotechnology, nanophotonics and biomedicine [1–5]. Unique optical properties of such nanoparticles arising from excitation of surface plasmon resonance [6] provide for a series of nonlinear effects (enhanced light absorbance, Raman scattering [7] and fluorescence [8]) and allow the multifold improvement of sensitivity of conventional analytical methods.

Practical application of the noble metals nanoparticles requires the possibility of targeted tuning of the position and intensity of the surface plasmon resonance maximum: for example, the nanoparticles to be used in biomedicine should exhibit the plasmon resonance in the "transparency window" of the studied tissue at the fluorescence maximum of the used probe or in the laser excitation range. Tuning of the surface plasmon resonance is important for development of highly sensitive method of absorption (nano) spectroscopy based on the effect of plasmon resonance energy transfer [9]: partial transfer of the excited plasmon energy to the analyte molecules located on the surface of the metal nanoparticles or in its vicinity. The spectrum of resonance light scattering of the nanoparticles exhibits the dips at the wave-lengths corresponding to the absorption maxima of the analyzed compounds. Resonance transfer of energy is short-range process and is much more efficient than the optical absorbance. The key condition for the transfer of plas-mon resonance energy is the overlap between surface plasmon resonance and absorption bands of the analyzed compound.

Position of the surface plasmon resonance is determined by the metal nature as well as the shape, the size and the structure of the nanoparticles [1–6, 9, 10]. However, the fine tuning of surface plasmon resonance over the wide spectral range using a single metal is seriously limited. In this regard, the bimetallic core-shell nanocomposites are promising, since the resonance optical properties of such materials depend on the core size and the shell thickness. For instance, the plasmon resonance of the Au/Ag nanocomposite can be fine-tuned over a broad spectral range [10–14].

Spherical core-shell nanocomposites have been prepared via precipitation of silver onto gold nanoparticles [10]; surfactants and polymers have been used in some procedures. The simplest approach is the reduction of one of the metal on the surface of the other one, the formed particles being stabilized with citrate or a polymer [11]. Prior to coating with silver,

Table 1. Spectral parameters of gold nanoparticles

Reaction mixture		Isolated nanoparticles		
λ_{max}, nm	diameter, nm	medium	λ_{max}, nm	diameter, nm
536	50	0.3 mmol/L of sodium citrate	661	~300
527	31	50 vol % of ethanol, 0.5 mmol/L of sodium citrate	577	132

gold nanoparticles can be modified with thiolated DNA [12], polyethylene glycol [13], or incorporated into polyelectrolyte multilayer of polydiallyldimethylammonium chloride and polystyrenesulfonate [14].

This work aimed to develop a procedure to prepare the Au/Ag composite in a 1 : 1 water–ethanol mixture and to demonstrate the product application in highly sensitive absorption spectroscopy based on plasmon resonance energy transfer.

Chemical reduction of a mixture of gold and silver salts results in fused bimetallic particles [10]. Therefore, the core-shell Au/Ag composite should be prepared in two stages: synthesis of gold nanoparticles followed by their coating with silver [10]. Intensity of light scattering with monometallic nanoparticles is known to be enhanced with increased particles diameter [15]. However, in the case of the Au/Ag composite, increase in the total nanoparticle size with simultaneous decrease of the ratio between the silver layer thickness and the gold core diameter has been accompanied by slight shift of the surface plasmon resonance maximum [16]. In view of this, the targeted stepwise synthesis of the Au/Ag composite requires optimization of the conditions of preparation of both the gold core and the silver shell.

Synthesis of gold nanoparticles in the water–ethanol mixture. In order to test the necessity of the gold nanoparticles purification during the Au/Ag composite synthesis, we compared the size of the prepared gold nanoparticles in the reaction mixture and after the isolation (Table 1). Centrifugation of the gold sol yielded large agglomerates both in the aqueous solution of sodium citrate (~300 nm) and in the water–ethanol mixture (132 nm). Therefore, the stage of the gold nanoparticles purification was excluded from the procedure of the Au/Ag composite synthesis.

Reduction of $HAuCl_4$ in the 1 : 1 water–ethanol mixture was accompanied by enhancement of the gold nanoparticles absorption, shifting of the surface plasmon resonance maximum and the change in the particles size (Fig. 1). However, the latter two parameters increase only at the $HAuCl_4$ concentration of 0.05 to 0.20 mmol/L, decreasing again at a higher concentration. The gold nanoparticles size is known to be a function of the [sodium citrate]/[$HAuCl_4$] ratio: the synthesis in water in a huge excess of sodium citrate yields the smaller gold nanoparticles [17]. The condensation methods of metal colloids preparation are based on generation of high supersaturation with respect to the metal atoms [17]. At the lower concentration of $HAuCl_4$ (0.05–0.20 mmol/L), the new phase formation is determined by the sodium citrate excess (5–20-fold) allowing for the fast supersaturation of the medium with Au^0. Gold atoms are disposed of the formation of the interatomic linkages [18]. That process was the driving force of condensation of a new phase, gold nanoparticles (<2 nm), in the discussed experiment; the latter were unstable towards aggregation in the water–ethanol medium and hence readily coagulated to yield the larger particles (up to ~140 nm) (Fig. 1b). At the smaller excess of sodium citrate (<5-fold), its coagulation efficiency was reduced but the rate of Au^0 formation remained high and the formed sol contained predominantly the smaller gold nanoparticles. At all $HAuCl_4$ concentrations (Fig. 1), the excess of sodium citrate (1.7–13.3-fold) was above the stoichiometric ratio (1.5-fold) of reaction (1).

$$2HAuCl_4 + 3Na_3C_6H_5O_7 = 2Au + 3Na_2C_5H_4O_5 + 3CO_2 + 3NaCl + 5HCl. \quad (1)$$

It should be noted that the excess of sodium citrate does not affect the completeness of $HAuCl_4$ reduction [17]. The highest content of gold nanoparticles was attained at 0.4 mmol/L of $HAuCl_4$, therefore that concentration was used in further experiments. Under these conditions the gold nanoparticles were of 78±17 nm as calculated via the $d = 2.02X - 23.1$ equation with $X = \lambda_{max} - 500$ [15].

More monodisperse nanoparticles can be prepared in the presence of polymer [10, 19]. In this regard, we studied the influence of a polycations (polyethyleneimine), polyanions (carboxymethylcellulose and polystyrenesulfonate) and nonionic polymers (dextran,

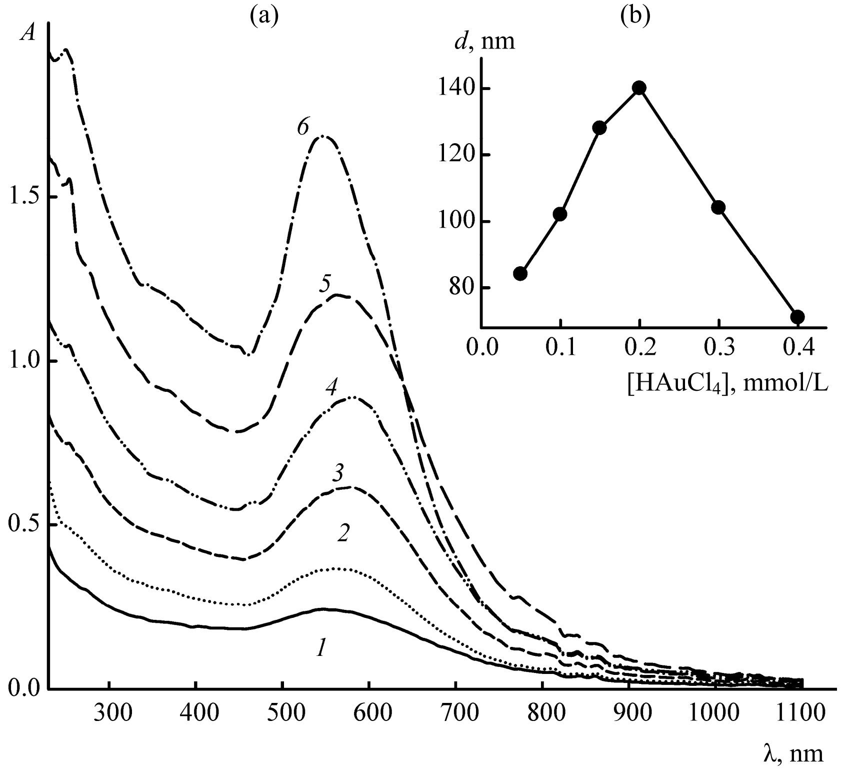

Fig. 1. (a) Extinction spectra of gold nanoparticles prepared at $HAuCl_4$ concentration of (*1*) 0.05, (*2*) 0.10, (*3*) 0.15, (*4*) 0.20, (*5*) 0.30, and (*6*) 0.40 mmol/L in the 1 : 1 water–ethanol mixture containing 1.0 mmol/L of sodium citrate; (b) diameter of the gold nanoparticles as a function of the initial $HAuCl_4$ concentration.

polyethyleneglycol and poly-*N*-vinylpyrrolidone) on the synthesis of gold nanoparticles in the 1 : 1 water–ethanol mixture. In the presence of dextrans T110 and T500 (poorly soluble in the solvent used), gray-violet gold sol was formed. The extinction spectrum of this product does not contain a distinct plasmon band of gold (Fig. 2a, spectrum *1*). Evidently, the gold nanoparticles linked the dextran aggregates of variable size. In contrast to the dextrans cases, polyethylene glycol was readily soluble in the solvent and formed the violet-pink gold sol (the extinction maximum of 536 nm, Fig. 3a, spectrum *1*) was formed in the presence of 0.15 mg/mL of polyethylene glycol. The product spectrum exhibited a ≈13 nm blue shift as compared to the spectrum of the sol prepared in the absence of the polymer.

The spectrum of the gold nanoparticles prepared in the presence of the above-named anionic polymers exhibited the red shift as compared to the spectrum of the sol prepared in the absence of polymer. The most prominent shift was observed in the case of polystyrenesulfonate additive (~100 nm) (Fig. 2a, spectrum *2*).

Similarly to the dextrans, polyethyleneimine was not an efficient additive in the gold nanoparticles synthesis: its solubility in the studied solution was significantly reduced in the presence of 1.0 mmol/L of sodium citrate. Moreover, gold nanoparticles formed poorly soluble aggregates with polyethyleneimine. Under the studied conditions, only poly-*N*-vinylpyrrolidone allowed synthesis of the non-agglomerated 13–20 nm spherical gold nanoparticles (Fig. 2c) absorbing at 524–528 nm (Fig. 2a, spectrum *3*).

Poly-*N*-vinylpyrrolidone and polyethylene glycol were the most efficient additives in the synthesis of gold nanoparticles. These polymers practically did not influence the gold nanoparticles extinction (Fig. 3a) but noticeably changed the particles size (Fig. 3b). In the absence of any polymer, the gold nanoparticles of ≈76 nm in diameter were formed. In the presence of 0.05 and 0.10 mg/mL of polyethylene glycol, the particles size was increased to 219 and 225 nm, respectively being down to 50–84 nm in the presence of 0.15–0.30 mg/mL of the polymer (Fig. 3b, curve *1*). Similar behavior was observed in the case of poly-*N*-vinylpyrrolidone (Fig. 3b, curve *2*). The smallest gold

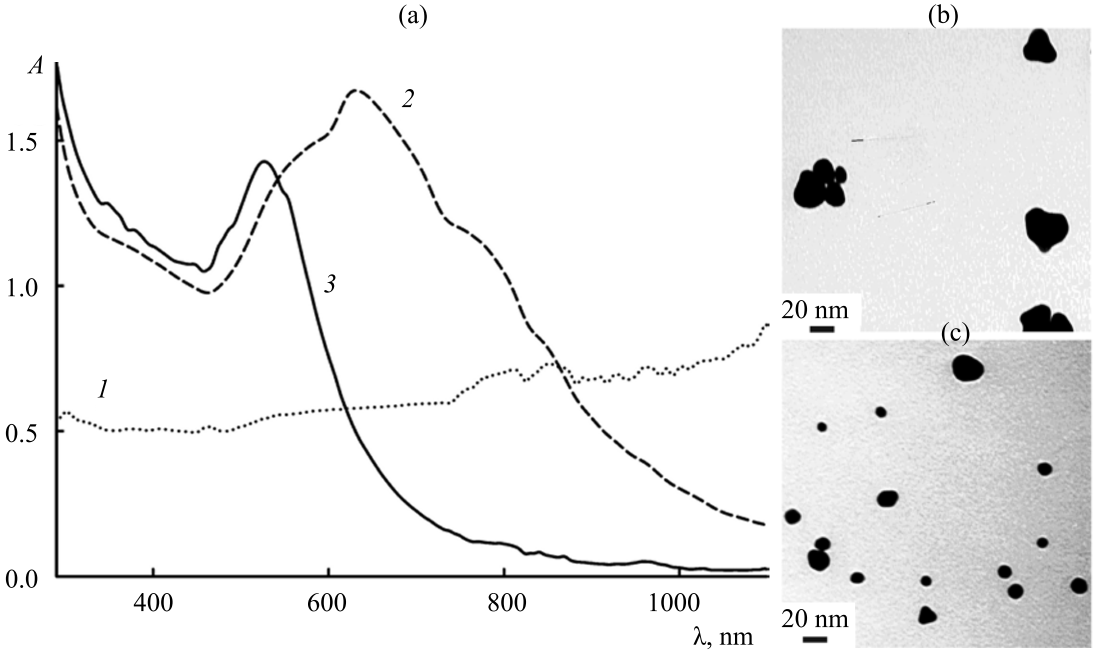

Fig. 2. (a) Extinction spectra of gold nanoparticles prepared in the 1 : 1 water–ethanol mixture containing 0.4 mmol/L of $HAuCl_4$, 1.0 mmol/L of sodium citrate, and 0.15 mg/mL of (*1*) poly-*N*-vinylpyrrolidone (24 kDa), (*2*) dextran T110, or (*3*) sodium polystyrenesulfonate; (b) TEM images of the particles prepared in the polymer-free medium and (c) in the presence of poly-*N*-vinylpyrrolidone (40 kDa).

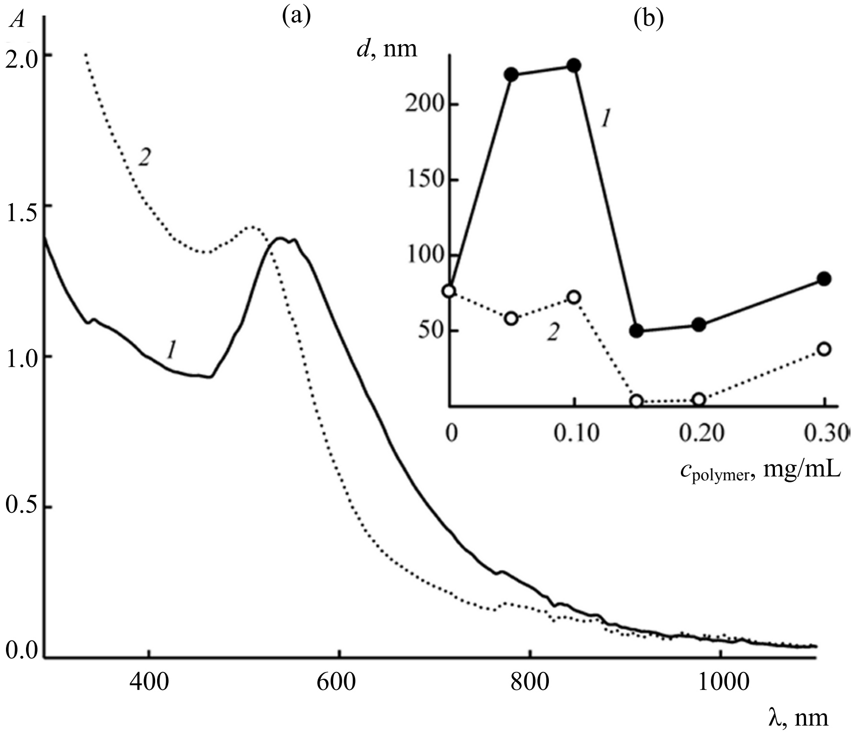

Fig. 3. (a) Extinction spectra of gold nanoparticles prepared in the 1 : 1 water–ethanol mixture containing 0.4 mmol/L of $HAuCl_4$, 1.0 mmol/L of sodium citrate, and 0.2 mg/mL of (*1*) polyethylene glycol or (*2*) poly-*N*-vinylpyrrolidone (40 kDa); (b) the gold nanoparticles diameter as a function of the polymer concentration in the reaction medium: (*1*) polyethylene glycol and (*2*) poly-*N*-vinylpyrrolidone (40 kDa).

nanoparticles (3–4 nm in diameter) forming a stable sol were obtained in the presence of 0.15 and 0.20 mg/mL of poly-*N*-vinylpyrrolidone (Fig. 3b). The data evidenced the dual effect of polyethylene glycol and poly-*N*-vinylpyrrolidone on the stability of the gold nanoparticles sol against aggregation in the 1 : 1 water–ethanol mixture containing sodium citrate. At the concentration below 0.1 mg/mL, those polymers acted jointly with sodium citrate, stimulating the gold sol flocculation. The highest flocculation activity was revealed in the case of polyethylene glycol (Fig. 3b, curve *1*). At the concentration above 0.1 mg/mL, the polymers acted as colloid stabilizers. Likely, the macromolecules completely coated the gold nanoparticles protecting the sol against aggregation. Poly-*N*-pyrrolidone was further used as additive for synthesis of gold nanoparticles; the size of the so prepared particles was 13±5 nm (Fig. 3b, curve *2*).

Coating of gold nanoparticles with silver. The gold nanoparticles were layered with silver in the presence of hydrogen peroxide capable of dissolution of free silver nanoparticles being inert towards gold nanoparticles [20]. Extinction spectrum of the Au/Ag composite prepared in the 1 : 1 water–ethanol medium in the presence of 0.05–0.30 mmol/L of $AgNO_3$ and in the absence of any polymer did not contain distinct plasmon bands of gold or silver (Fig. 4a, spectrum *1*). Increasing the $AgNO_3$ content in the mixture resulted exclusively in the stronger absorption at 290–1100 nm. The Au/Ag sol exhibited low colloid stability in the reaction mixture.

The maximum of the surface plasmon resonance of the gold nanoparticles prepared in the presence of poly-*N*-vinylpyrrolidone (340 kDa) and various concentration of $AgNO_3$ was shifted towards short wavelength, the surface plasmon resonance of both gold and silver components growing stronger (Fig. 4). Those changes evidenced the formation of the Au/Ag composite containing varied amount of silver at the gold core surface. When the silver shell was thicker than 3 nm, the surface plasmon resonance of the gold core was completely screened and the extinction spectrum contained only the silver bands [21]. The Au/Ag composite of the core–satellite type was likely formed at $AgNO_3$ concentration below 0.6 mmol/L, since the extinction spectrum contained the bands of surface plasmon resonance of both silver and gold (Fig. 4a).

It is noteworthy that the TEM images of the Au/Ag composite revealed the presence of agglomerates when the particles were prepared in the polymer-free mixtures or in the presence of carboxymethylcellulose, dextran T110, or polystyrenesulfonate. The agglomeration was less prominent when the Au/Ag composite was prepared in the presence of poly-*N*-vinylpyrrolidone (40 or 360 kDa; in the latter case, the average size of the composite particles was of 14±3 nm, Fig. 5c).

Mean hydrodynamic diameter of the Au/Ag composite prepared in the polymer-free medium was noticeably higher than that of the products prepared in the presence of the polymers (Table 2). The composite nanoparticles diameter was decreased 2.7–4.7 times in the presence of carboxymethylcellulose, dextrans, or polystyrenesulfonate. However, the lowest hydrodynamic value (73–88 nm) was observed in the case of the Au/Ag composite formed in the presence of poly-*N*-vinylpyrrolidone (Table 2).

Hydrodynamic diameter of almost all Au/Ag particles formed in the presence of poly-*N*-vinylpyrrolidone (360 kDa) was 6–22 nm (Fig. 5b, curve *2*). These particles practically did not scatter light (Fig. 5a). The Au/Ag composite prepared in the presence of poly-*N*-vinylpyrrolidone (40 kDa) contained particles with diameter of 20 to 150 nm exhibiting stronger light scattering (Fig. 5a). It is presumable that poly-*N*-vinylpyrrolidone molecules are the substrate for the gold nanoparticles formation on their surface and then silver nanoparticles and clusters settled onto this surface. The polymer core size depended on the polymer molecular mass. Several macromolecules could possibly form the composite core in the cases of the shorter polymer chains (24 and 40 kDa), thus enhancing the Au/Ag particles polydispersity (Figs. 5a, 5b, curve *1*).

Resonance light scattering of the Au/Ag composite. The conditions of preparation of gold sols and Au/Ag composite were reflected in the formed particles size and, consequently, their ability to absorb and scatter light. The intensity of absorbance by the gold sol prepared in the 1 : 1 water–ethanol mixture was enhanced when the $HAuCl_4$ concentration in the reaction mixture increased from 0.05 to 0.40 mmol/L (Fig. 1a). At the same time, the gold sol with the particles diameter of 84–128 nm prepared via reduction of 0.05–0.15 mmol/L $HAuCl_4$ exhibited weak light scattering (Fig. 6a, curves *1* and *2*). Distinct resonance scattering spectrum with maximum at 667 nm was observed in the case of the sol with the particles diameter of 71 nm prepared via reduction of

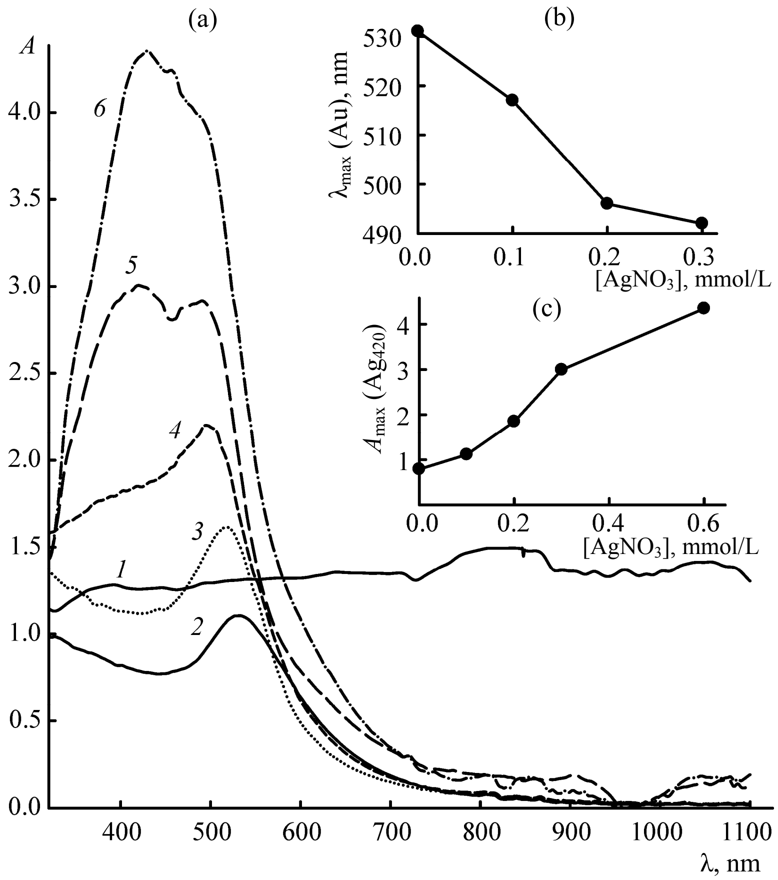

Fig. 4. (a) Extinction spectra of the Au/Ag composite (*1*, *3*–*6*) and the gold nanoparticles (*2*) prepared in the 1 : 1 water–ethanol mixture in the absence of a polymer and in the presence of 0.15 mg/mL of poly-*N*-vinylpyrrolidone (360 kDa) (*2*–*6*) during reduction of (*1*) 0.5, (*2*) 0, (*3*) 0.1, (*4*) 0.2, (*5*) 0.3, and (*6*) 0.6 mmol/L $AgNO_3$; (b) position of the maximum of gold surface plasmon resonance and (c) absorbance of silver at 420 nm as a function of $AgNO_3$ concentration during the Au/Ag composite formation.

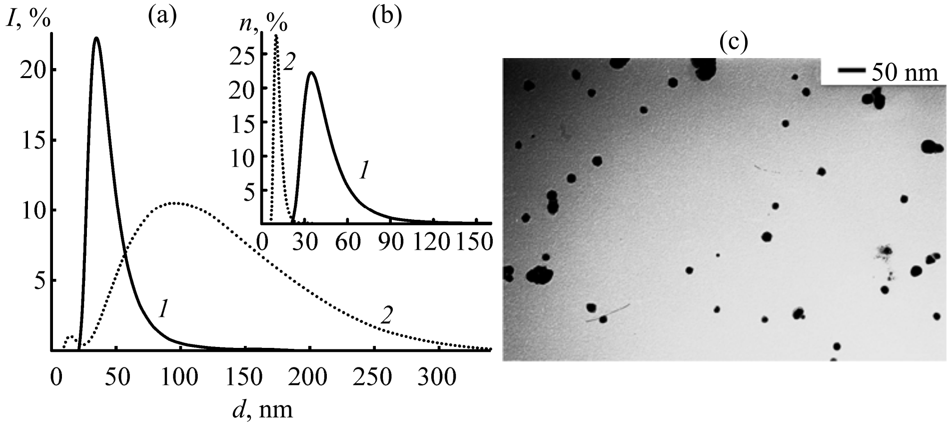

Fig. 5. (a) Distribution of light scattering intensity and (b) the particles number of the Au/Ag composite formed in the presence of (*1*) poly-*N*-vinylpyrrolidone (40 kDa) or (*2*) poly-*N*-vinylpyrrolidone (360 kDa); (c) TEM image of the Au/Ag composite formed in the presence of poly-*N*-vinylpyrrolidone (360 kDa) (scanning area 870×600 nm).

Table 2. Hydrodynamic parameters of the Au/Ag composite prepared in the presence of 0.11 mg/mL of different polymers

Additive	Zeta potential, mV	Conductivity, mS/cm	Mean diameter, nm	Polydispersity
Polymer-free	–15.1	0.021	767	0.392
Carboxymethylcellulose	–39.1	0.213	161	0.274
Poly-*N*-vinylpyrrolidone (40 kDa)	–33.8	0.117	88	0.262
Poly-*N*-vinylpyrrolidone (360 kDa)	–21.6	0.239	73	0.365
Dextran T110	–11.9	0.269	285	0.248
Dextran T500	–7.9	0.218	260	0.334
Sodium polystyrenesulfonate	–29.2	0.285	237	0.297

0.4 mmol/L of $HAuCl_4$ (Fig. 6a, curve *3*). The intensity of scattering with the Au/Ag composite was determined by the amount of silver settled on the gold core surface. The Au/Ag samples with the low fraction of silver prepared at 0.05 to 0.15 mmol/L of $AgNO_3$ showed weak light scattering (Fig. 6b, curves *1*–*3*). The strongest light scattering was observed for the samples containing higher silver fraction: those prepared via reduction of 0.2–0.3 mmol/L of $AgNO_3$ (Fig. 6b, curves *4*, *5*).

The Au/Ag composite prepared in the presence of polyethylene glycol or sodium polystyrenesulfonate revealed a broad scattering band at 650–800 nm (Fig. 7). The strongest scattering signal observed as the distinct peak was registered in the case of the Au/Ag composite prepared in the presence of poly-*N*-vinylpyrrolidone (Fig. 7). The location of the scattering band depended on the polymer molecular mass: the maximum was found at 605 nm in the case of 360 kDa poly-*N*-vinylpyrrolidone and at 576–579 nm when the polymer molecular mass was of 24 kDa or 40 kDa (Fig. 7).

In order to estimate the efficiency of the Au/Ag composite in absorption spectroscopy based on plasmon resonance energy transfer, we recorded the resonance scattering spectra of the sols in the presence of water-soluble cationic and anionic porphyrins. The spectrum of cationic Cu(II)-5,10,15,20-tetrakis(4-*N*-methylpyridinium)porphyrin (CuTMPyP4) contained the absorption band with the maximum at 550 nm (Fig. 8a, spectrum *1*), overlapping with the scattering band of the Au/Ag composite prepared in the presence

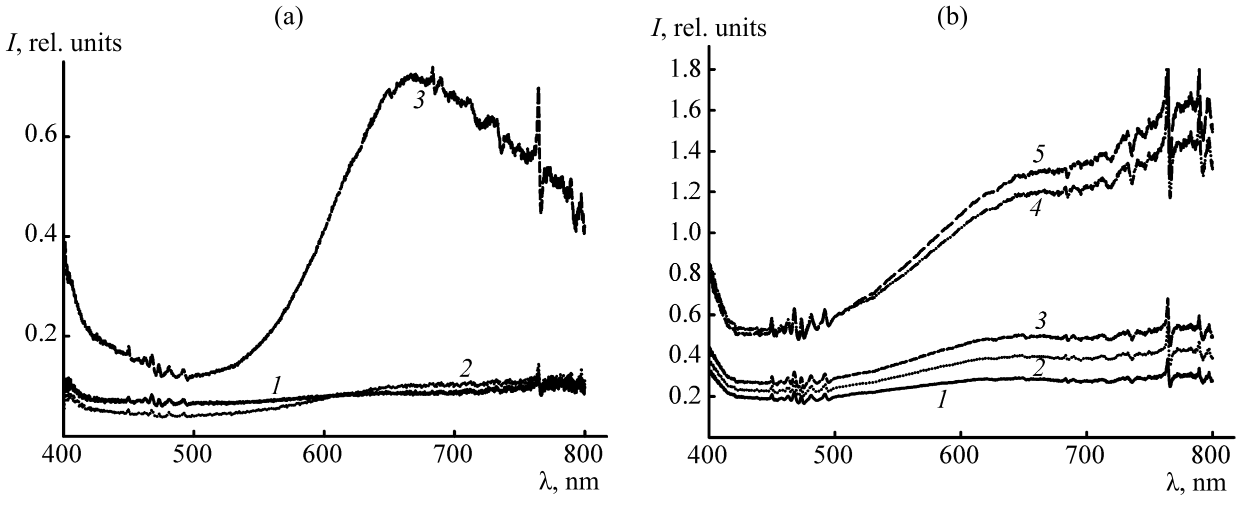

Fig. 6. (a) Scattering spectra of gold nanoparticles prepared in the 1 : 1 water–ethanol mixture containing 1.0 mmol/L of sodium citrate at $HAuCl_4$ of (*1*) 0.05, (*2*) 0.15, and (*3*) 0.40 mmol/L and (b) of the Au/Ag composite prepared at $AgNO_3$ concentration of (*1*) 0.05, (*2*) 0.10, (*3*) 0.15, (*4*) 0.20, and (*5*) 0.30 μmol/L in the absence of polymer.

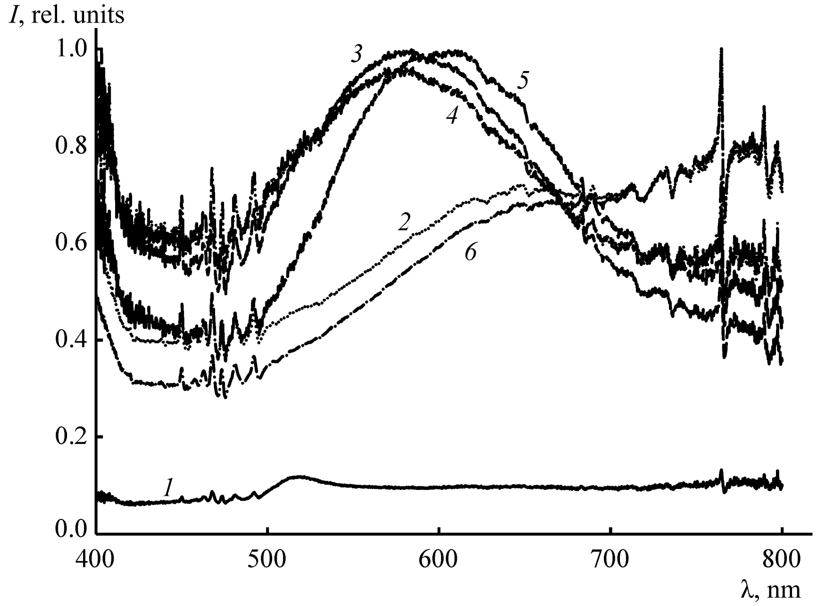

Fig. 7. Scattering spectra of the Au/Ag composites prepared in the presence of different polymers: (*1*) no polymer; (*2*) polyethylene glycol (4 kDa); (*3*) poly-*N*-vinylpyrrolidone (240 kDa); (*4*) poly-*N*-vinylpyrrolidone (40 kDa), (*5*) poly-*N*-vinylpyrrolidone (360 kDa); and (*6*) sodium polystyrenesulfonate.

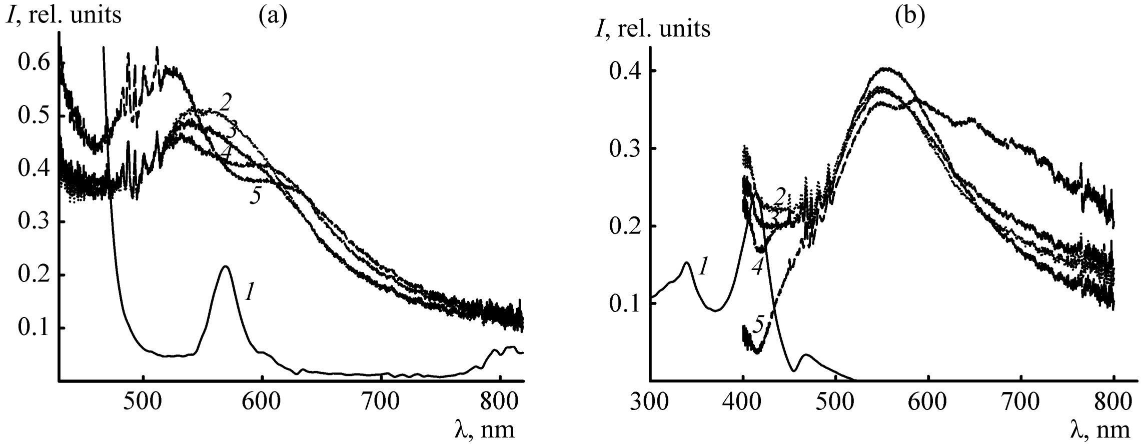

Fig. 8. Extinction spectra of the porphyrins (a): (*1*) 1.0 µmol/L of CuTMPyP4, (b) (*1*) 5.0 µmol/L of FeTPPS and (*2*) scattering spectra of the Au/Ag composite, its complex with CuTMPyP4 (a): (*3*) 0.1, (*4*) 0.4, and (*5*) 2.0 µmol/L or FeTPPS (b): (*3*) 1, (*4*) 10, and (*5*) 100 µmol/L.

of the 360 kDa poly-*N*-vinylpyrrolidone (Fig. 8a, spectrum *2*). Depending on the CuTMPyP4 concentration, the light scattering spectra showed the decreased intensity at 530 nm and the dips at about 560 nm, due to the transfer of the plasmon resonance energy of the Au/Ag composite at the CuTMPyP4 molecules (Fig. 8a). Addition of the anionic Fe-tetra-(sulfonatophenyl)porphyrin (FeTPPS) to the Au/Ag sol prepared in the presence of the 360 kDa poly-*N*-vinylpyrrolidone resulted in the appearance of the dips at 413–415 nm, coinciding with the position of strong Soret band of the porphyrin (Fig. 8b); that was likely due to the effect of the plasmon resonance energy transfer as well.

To summarize, the two-step synthesis carried out in this work in the 1 : 1 water–ethanol mixture yielded the Au/Ag composite suitable for application in absorption spectroscopy based on the plasmon resonance energy transfer. The presence of a polymer additive was a key factor to determine the synthesis outcome. The addition of poly-*N*-vinylpyrrolidone was the most efficient; spherical Au/Ag composite particles with narrow size distribution (14±3 nm) were formed in the presence of this polymer. Probably, the structures consisting of polymeric core coated with the Au/Ag nanoparticles were formed in the reaction mixture. Those structures exhibited strong light scattering and were capable of binding anionic as well as cationic porphyrins. Increasing the porphyrins concentration resulted in the appearance of the dips in the scattering spectra of Au/Ag, their positions coinciding with the absorption maximums of the porphyrins. The smooth shift of the maximums of the absorption (≈150 nm) and resonance scattering (≈84 nm) bands of the Au/Ag composite towards the shorter wavelength was attained by variation of the silver content on the surface of the gold core; the silver content was in turn determined by the concentration of silver nitrate in the reaction mixture in the second stage of the synthesis.

EXPERIMENTAL

The following commercially available chemicals were used: $HAuCl_4 \cdot 3H_2O$, carboxymethylcellulose (250 kDa), sodium polystyrenesulfonate (70 kDa), poly-*N*-vinylpyrrolidone (24, 40, and 360 kDa) (all from Sigma-Aldrich, USA); dextran T500 (Loba-Chemie, Austria); dextran T110 and polyethylene glycol (4 kDa) (both from Fluka, Switzerland); hydrogen peroxide (Belleskhimkomplekt, Belarus); sodium citrate, $AgNO_3$, $NaHCO_3$ and 25 wt% aqueous ammonia (all from Reakhim, Russia). Cu(II)-5,10,15,20-Tetrakis(4-*N*-methylpyridinium)porphyrin and Fe-tetra(sulfonatophenyl)porphyrin were prepared by V.L. Malinovskii (Bogatskii Physico-Chemical Institute, National Academy of Sciences, Ukraine).

Gold nanoparticles were prepared in the 1 : 1 water–ethanol mixture containing 0.3 mmol/L of $HAuCl_4$ and 1.0 mmol/L of sodium citrate under ultrasonication (an Elmasonic S30H bath, Germany) during 3 h at 16.0 to 62.0°C. The gold nanoparticles were isolated via centrifugation (Allegra 64R, Beckman, USA, 30 min, 20000 rpm) followed by washing with a water–ethanol mixture containing 0.5 mol/L of sodium citrate and dispersion in the same mixture.

Au/Ag composite was prepared in the 1 : 1 water–ethanol mixture in two steps: the gold nucleates were first formed and then modified with silver. The gold nucleates were prepared under ultrasonication (3 h) in 1.5 mL of the solution containing 0.4 mmol/L of $HAuCl_4$, 1.0 mmol/L of sodium citrate and 0.15 mg/mL of poly-*N*-vinylpyrrolidone. 0.5 mL of the solution containing $NaHCO_3$ (10 mmol/L) glucose (50 mmol/L), H_2O_2 (5.0 mmol/L) and $AgNO_3$ (0.25 mmol/L) were then added to 1.5 mL of the so prepared gold sol and the mixture was ultrasonicated during 3 h.

Absorbance spectra of gold nanoparticles and the Au/Ag composite were recorded using an SM 2203 spectrofluorimeter (Solar, Belarus) and a Cary 500 Scan spectrophotometer (Varian, USA). Size and shape of the nanoparticles were estimated from transmission electron microscopy (JEM-100CX, Japan) and atomic force microscopy (Nanoscope-3D, Veeca, USA) data. Zeta potential and hydrodynamic diameter of the nanoparticles were determined using a Zetasizer Nano instrument (Malvern Instruments, Great Britain).

Resonance scattering spectra were recorded using a single-beam experimental unit [22–24]. Strong absorption by the metal nanoparticles near the surface plasmon resonance maximum could significantly distort the resonance scattering bands; therefore, the real bands shape was determined using the following correction equation [24]:

$$I_{\mathrm{real}}(\lambda) = I_{\mathrm{sc}}(\lambda)/\{10\times[-n\cdot \mathrm{Abs}(\lambda)/m]\},$$

with $I_{\mathrm{real}}(\lambda)$ and $I_{\mathrm{sc}}(\lambda)$ being the corrected and the measured resonance scattering intensity, respectively; Abs(λ) being the absorbance of the nanoparticles in the solution; *m* being the dilution factor; *n* being the constant determined by the geometry of the exciting irradiation and the measured scattering intensity. The *n* value was calculated from the spectra of resonance scattering measured for a series of gold nanoparticles solutions at the up to 100-fold dilution. The *n* factor was then fitted so that the scattering band shape was identical for all the samples, coinciding with that for the diluted solutions (with the absorbance below 0.1). For the used single-beam setup, the *n* value was 0.5–0.7.

REFERENCES

1. Khlebtsov, N.G. and Dykman, L.A., *J. Quant. Spectroscopy & Radiative Transfer.*, 2010, vol. 111, no. 1, p. 1. DOI: 10.1016/j.jqsrt.2009.07.012.
2. Jain, P.K., Huang, X.H., El-Sayed, I.H., and El-Sayed, M.A., *Acc. Chem. Res.*, 2008, vol. 41, no. 12, p. 1578. DOI: 10.1021/ar7002804.

3. Khlebtsov, N.G., *Kvant. Elektron*., 2008, vol. 38, no. 6, p. 504.
4. Anker, J.N., Hall, W.P., Lyandres, O., Shah, N.C., Zhao, J., and Van Duyne, R.P., *Nat. Mater*., 2008, vol. 7, no. 6, p. 442. DOI: 10.1038/nmat2162.
5. Rosi, N.L. and Mirkin, C.A., *Chem. Rev*., 2005, vol. 105, no. 4, p. 1547. DOI: 10.1021/cr030067f.
6. Kreibig, U. and Vollmer, M., *Optical Properties of Metal Clusters. Springer Series in Materials Science*, Heidelberg: Springer, 1995, vol. 25.
7. Kneipp, K., Kneipp, H., Itzkan, I., Dasari, R.R., and Feld, M.S., *Chem. Rev*., 1999, vol. 99, no. 10, p. 2957. DOI: 10.1021/cr980133r.
8. Kulakovich, O., Strekal, N., Yaroshevich, A., Maskevich, S., Gaponenko, S., Nabiev, I., Woggon, U., and Artemyev, M., *Nano Lett.*, 2002, vol. 2, no. 12, p. 1449.
9. Liu, G.L., Long, Y.-T., Choi, Y., Kang, T., and Lee, L.P., *Nature Methods*, 2007, vol. 4, no. 12, p. 1015. DOI: 10.1038/nmeth1133.
10. Toshima, N. and Yonezawa, T., *New J. Chem*., 1998, vol. 22, no. 11, p. 1179. DOI: 10.1039/A805753B.
11. Samal, A.K., Polavarapu, L., Rodal-Cedeira, S., Liz-Marzán, L.M., Pérez-Juste, J., and Pastoriza-Santos, P., *Langmuir*, 2013, vol. 29, no. 48, p. 15076. DOI: 10.1021/la403707j.
12. Lim, D.-K., Kim, I.-J., and Nam, J.-M., *Chem. Commun*., 2008, no. 42, p. 5312. DOI: 10.1039/B810195G.
13. Sánchez-Iglesias, A., Carbó-Argibay, E., Glaria, A., Rodríguez-González, B., Pérez-Juste, J., Pastoriza-Santos, I., and Liz-Marzán, L.M., *Chem. Eur. J*., 2010, vol. 16, no. 19, p. 5558. DOI: 10.1002/chem.201000144.
14. Zhang, X., Wang, H., and Su, Z., *Langmuir*, 2012, vol. 28, no. 44, p. 15705. DOI: 10.1021/la303320z.
15. Khlebtsov, N.G., Bogatyrev, V.A., Dykman, L.A., and Khlebtsov, B.N., *Ross. Nanotekhnol*., 2007, vol. 2, nos. 3–4, p. 69.
16. Steinbrück, A., Csáki, A., Festag, G., and Fritzsche, W., *Plasmonics*., 2006, vol. 1, no. 1, p. 79. DOI: 10.1007/s11468-005-9000-5.
17. Dykman, L.A., Bogatyrev, I.A., Shchegolev, S.Yu., and Khlebtsov, N.G., *Zolotye nanochastitsy: sintez, svoistva, biomeditsinskoe primenenie* (Gold Nanoparticles: Synthesis, Properties, and Biomedical Applications), Moscow: Nauka, 2008.
18. Paddefet, R., *Khimiya zolota* (Chemistry of Gold), Moscow: Mie, 1982.
19. Pomogailo, A.D., Rozenberg, A.S., and Uflyand, I.E., *Nanochastitsy metallov v polimerakh* (Metal Nanoparticles in Polymers), Moscow: Khimiya, 2000.
20. Zhang, Q., Li, N., Goebl, J., Lu, Z., and Yin, Y., *J. Am. Chem. Soc*., 2011, vol. 133, no. 46, p. 18931. DOI: 10.1021/ja2080345.
21. Ma, Y., Li, W., Cho, E.C., Li, Z., Yu, T., Zeng, J., Xie, Z., and Xia, Y., *AcsNano*, 2010, vol. 4, no. 11, p. 6725. DOI: 10.1021/nn102237c.
22. Eryomin, A.N., Abakshonok, A.V., Agabekov, V.E., Gracheva, E.A., Zhavnerko, G.K., Terekhov, S.N., and Panarin, A.Yu., *Dokl. Nats. Akad. Nauk Belarusi*, 2012, vol. 56, no. 6, p. 62.
23. Eryomin, A.N., Abakshonok, A.V., Agabekov, V.E., Zhavnerko, G.K., Panarin, A.Yu., and Terekhov, S.N., *Vestsi Nats. Akad. Nauk Belarusi*, *Ser. Khim. Navuk*, 2013, no. 1, p. 55.
24. Panarin, A.Yu., Abakshonok, A.V., Agabekov, V.E., Eryomin, A.N., and Terekhov, S.N., *Zh. Prikl. Spektr*., 2014, vol. 81, no. 6, p. 940.